

Low-Energy Electron Diffraction Intensities: Comparison between Theory and Experiment*

F. HOFMANN† AND HAROLD P. SMITH, JR.‡

Space Sciences Laboratory and Department of Nuclear Engineering, University of California, Berkeley, California 94720

(Received 26 November 1968; revised manuscript received 2 September 1969)

An extended version of the Bethe theory of low-energy electron diffraction is presented and successfully applied to a computation of diffracted beam intensity as a function of wavelength of the incident electron. The results show consistent behavior with respect to parameter variation and are in reasonable agreement with measured beam intensities.

I. INTRODUCTION

IT is generally agreed that, up to the present time, the use of low-energy electron diffraction (LEED) as a tool for surface-structure analysis has met with only partial success, due to the lack of a sufficiently accurate, numerically tractable, theoretical model. Thus, it has not been possible to exploit fully the rapidly accumulating experimental information, especially beam intensity measurements.

Recently, a number of theoretical treatments of LEED have been proposed. They may be divided into two categories, i.e., kinematical and dynamical theories. In the former, as in x-ray diffraction theory, multiple scattering is neglected, whereas in the latter, this phenomenon is treated more or less rigorously. Several authors have shown,¹⁻³ however, that multiple scattering is a vitally important process in LEED and that only the dynamical theories may be able to explain in detail the dependence of the beam intensities on electron energy.

Dynamical effects in LEED have been investigated by a number of authors,³⁻⁹ using various models, methods, and approximations. Our method⁶ is based on the Bethe theory¹⁰ which assumes that the incident and the diffracted electron beams are plane waves and that the crystal can be represented by a three-dimensional periodic potential, cut off abruptly at a plane surface.

The present paper consists of three parts: first, a brief review of the theory (Secs. II-IV), then a discussion of

the results of beam intensity calculations for an fcc lattice¹¹ (Sec. V), and finally, a comparison with recent experimental results¹² (Sec. VI).

II. MODEL

Let us consider a perfect crystal, represented by a complex periodic potential

$$W(\mathbf{r}) = \sum_{l,m,n} e^{2\pi i \mathbf{b}_{l,m,n} \cdot \mathbf{r}} w_{l,m,n}, \quad (z < 0) \quad (1)$$

$$W(\mathbf{r}) = 0, \quad (z \geq 0)$$

where $\mathbf{b}_{l,m,n}$ is the reciprocal lattice vector [e.g., in a cubic lattice, $\mathbf{b}_{l,m,n} = (1/a)(l, m, n)$, a being the lattice constant in real space].

The real part of $W(\mathbf{r})$ gives rise to elastic scattering, whereas the imaginary part causes electron "absorption" and, thus, phenomenologically accounts for inelastic processes.

The wave function in the vacuum, $\Phi(\mathbf{r})$, $z > 0$, is assumed to be the sum of an incident plane wave $e^{i\mathbf{K} \cdot \mathbf{r}}$, whose amplitude is equal to unity, and all possible diffracted plane waves $\Phi_{l,m} e^{i\mathbf{h}_{l,m} \cdot \mathbf{r}}$.

It can be shown¹⁰ that the propagation vectors of the diffracted beams are determined by

$$\mathbf{h}_{l,m\parallel} = \mathbf{K}_{\parallel} + 2\pi \mathbf{b}_{l,m}, \quad \mathbf{h}_{l,m\perp} = + (K^2 - h_{l,m\parallel}^2)^{1/2}, \quad (2)$$

where the subscripts \parallel and \perp indicate vector components parallel and perpendicular to the crystal surface, respectively, and $\mathbf{b}_{l,m} = \mathbf{b}_{l,m,n_{11}}$.

Thus, the wave function in the vacuum is written as

$$\Phi(\mathbf{r}) = e^{i\mathbf{K} \cdot \mathbf{r}} + \sum_{l,m} \Phi_{l,m} e^{i\mathbf{h}_{l,m} \cdot \mathbf{r}}. \quad (3)$$

III. PROBLEM

The mathematical problem may now be stated as follows: The one-electron Schrödinger equation $\nabla^2 \psi + (K^2 + W)\psi = 0$, with K^2 and W prescribed, is to be solved in the half-space $z < 0$ (i.e., within the crystal),

* Work partially supported by the NASA Ames Research Center, under Grant No. NGR-05-003-275.

† Present address: Centre de Recherches en Physique des Plasmas, Lausanne, Switzerland.

‡ Present address: Department of Applied Science, University of California, Davis/Livermore, Calif.

¹ E. G. McRae and C. W. Caldwell, *Surface Sci.* **2**, 509 (1964).

² G. Gafner, *Surface Sci.* **2**, 534 (1964).

³ E. G. McRae, *J. Chem. Phys.* **45**, 3258 (1966).

⁴ K. Hirabayashi and Y. Takeishi, *Surface Sci.* **4**, 150 (1966).

⁵ D. S. Boudreaux and V. Heine, *Surface Sci.* **8**, 426 (1967).

⁶ F. Hoffmann and Harold P. Smith, Jr., *Phys. Rev. Letters*, **19**, 1472, (1967).

⁷ P. M. Marcus and D. W. Jepsen, *Bull. Am. Phys. Soc.* **13**, 367 (1968).

⁸ K. Hirabayashi, *J. Phys. Soc. Japan* **24**, 846 (1968).

⁹ R. M. Stern, J. J. Perry, and D. S. Boudreaux, *Rev. Mod. Phys.* **41**, 275 (1969).

¹⁰ H. Bethe, *Ann. Physik* **87**, 55 (1928).

¹¹ E. C. Snow, *Phys. Rev.* **158**, 683 (1967).

¹² S. M. Bedair (private communication).

subject to the following boundary conditions:

- (1) $|\psi|^2$ finite for $z < 0$;
- (2) $\lim_{z \rightarrow -\infty} |\psi|^2 = 0$;
- (3) continuity of the wave function and its derivative with respect to the surface normal, at the surface, i.e., $\psi = \Phi$ and $\partial\psi/\partial z = \partial\Phi/\partial z$ at $z=0$, where Φ is given by Eq. (3).

The unknowns are the intensities of the diffracted beams, i.e., the amplitudes $\Phi_{l,m}$, and the wave function in the crystal, $\psi(\mathbf{r})$.

IV. METHOD OF SOLUTION

A. Bethe Equations

We assume the ansatz for the wave function used by Bethe,¹⁰

$$\psi(\mathbf{r}) = \sum_{l,m,n,s} e^{i\mathbf{k}_{l,m,n,s} \cdot \mathbf{r}} \psi_{l,m,n,s}, \quad (4)$$

where $\mathbf{k}_{l,m,n,s} = \mathbf{K}_{11} + \mathbf{s} + 2\pi\mathbf{b}_{l,m,n}$, $\mathbf{s} = (0,0,s)$, and s is a complex number. Note that the summation over s does not imply a double sum over its real and imaginary parts. These two quantities cannot be chosen independently because s must be a solution of the eigenvalue equation (5), below.

Combining (4) with the Schrödinger equation yields the well-known Bethe equation,

$$\psi_{l,m,n,s} (K^2 - k_{l,m,n,s}^2) + \sum_{l',m',n'} w_{l',m',n'} \psi_{l'-l',m'-m',n'-n',s} = 0, \quad (5)$$

where $k_{l,m,n,s}^2$ is the sum of the squares of the three components of the vector $\mathbf{k}_{l,m,n,s}$ (i.e., a complex number). Equation (5) may be regarded as an eigenvalue equation where s , contained in $k_{l,m,n,s}^2$, is the eigenvalue and $\psi_{l,m,n,s}$ is the corresponding eigenvector. Obviously, the complete solution of the problem consists of a superposition of the various eigenvectors, weighted by coefficients which are determined by invoking the boundary conditions. Many attempts^{5,7,9} have been made to solve this formidable problem. We will not try to solve it here. Instead, we are considering what might be called the "single-Bloch-wave approximation," i.e., we are looking for the dominant eigenvector and its eigenvalue.

B. Single-Bloch-Wave Approximation

Let us consider, for a moment, the case where $W(\mathbf{r}) = w_{0,0,0} = \text{const}$. Here, the solution is trivial. The wave function in the crystal consists of a single plane wave $e^{i\mathbf{K}_0 \cdot \mathbf{r}}$ whose propagation vector $\mathbf{K}_0 = (K_{0x}, K_{0y}, K_{0z})$ satisfies the following relations:

$$-(K_{0x}^2 + K_{0y}^2 + K_{0z}^2) + K^2 + w_{0,0,0} = 0 \quad (\text{Schrödinger equation});$$

$$\text{Im} K_{0x} = \text{Im}(K_{0y}) = 0, \quad \text{Im}(K_{0z}) < 0 \quad (\text{boundary conditions});$$

$$\text{Re}(K_{0z}) < 0$$

(beam traveling in the negative z direction).

It follows immediately from the above that $\text{Im}(w_{0,0,0}) > 0$. Furthermore, the "eigenvalue" s_0 may be computed by setting $\mathbf{K}_0 = \mathbf{k}_{l_0, m_0, n_0, s_0}$:

$$s_0 = K_{0z} - n_0 p = -(K_{11}^2 + w_{0,0,0})^{1/2} - n_0 p, \quad (6)$$

where p is the reciprocal lattice constant in the z direction (in a cubic lattice, $p = 2\pi/a$). In deriving (6) we have assumed that $l_0 = m_0 = 0$, and n_0 is chosen such that $0 < \text{Re}(K_{0z}) - n_0 p \leq p$. Equation (6) may be split into real and imaginary parts:

$$\begin{aligned} \text{Re}(s_0) \equiv q_0 &= (-1/\sqrt{2})(K_{11}^2 + \text{Re}(w_{0,0,0}) \\ &+ \{[K_{11}^2 + \text{Re}(w_{0,0,0})]^2 + \text{Im}(w_{0,0,0})^2\}^{1/2})^{1/2} - n_0 p, \\ \text{Im}(s_0) \equiv l_0 &= (-1/\sqrt{2})(-K_{11}^2 - \text{Re}(w_{0,0,0}) \\ &+ \{[K_{11}^2 + \text{Re}(w_{0,0,0})]^2 + \text{Im}(w_{0,0,0})^2\}^{1/2})^{1/2}. \end{aligned} \quad (6')$$

We now make the assumption that $s = s_0$, even in the case when $W(\mathbf{r}) \neq \text{const}$.

The quantity s is therefore a fixed number and no longer an eigenvalue parameter. Consequently, Eqs. (4) and (5) are rewritten as

$$\psi(\mathbf{r}) = \sum_{l,m,n} e^{i\mathbf{k}_{l,m,n} \cdot \mathbf{r}} \psi_{l,m,n}, \quad (4')$$

$$\begin{aligned} \psi_{l,m,n} (K^2 - k_{l,m,n}^2) \\ + \sum_{l',m',n'} w_{l',m',n'} \psi_{l-l',m-m',n-n'} = 0, \end{aligned} \quad (5')$$

where

$$\mathbf{k}_{l,m,n} = \mathbf{K}_{11} + \mathbf{s}_0 + 2\pi\mathbf{b}_{l,m,n}.$$

C. Boundary Conditions

The wave function (4') satisfies the first and second boundary conditions (Sec. III) if $\text{Im}(s_0) \equiv l_0 < 0$. It also satisfies the third boundary condition if

$$\sum_{l,m,n} e^{i\mathbf{k}_{l,m,n} \cdot \mathbf{r}} \psi_{l,m,n} = e^{i\mathbf{K} \cdot \mathbf{r}} + \sum_{l,n} e^{i\mathbf{h}_{l,m} \cdot \mathbf{r}} \Phi_{l,m} \quad (7)$$

and

$$\begin{aligned} \sum_{l,m,n} (\mathbf{k}_{l,m,n} \cdot \mathbf{1}_z) e^{i\mathbf{k}_{l,m,n} \cdot \mathbf{r}} \psi_{l,m,n} \\ = (\mathbf{K} \cdot \mathbf{1}_z) e^{i\mathbf{K} \cdot \mathbf{r}} + \sum_{l,m} (\mathbf{h}_{l,m} \cdot \mathbf{1}_z) e^{i\mathbf{h}_{l,m} \cdot \mathbf{r}} \Phi_{l,m} \end{aligned} \quad (8)$$

at the surface ($z=0$), where $\mathbf{1}_z$ is a unit vector in the z direction. Equations (7) and (8) may be decomposed into a set of equations relating the coefficients of the various harmonics in x and y :

$$\begin{aligned} \sum_n \psi_{l,m,n} &= \Phi_{l,m}, \quad (l \neq 0 \text{ or } m \neq 0) \\ \sum_n \psi_{0,0,n} &= \Phi_{0,0} + 1, \end{aligned} \quad (9)$$

$$\sum_n (\mathbf{k}_{l,m,n} \cdot \mathbf{1}_z) \psi_{l,m,n} = (\mathbf{h}_{l,m} \cdot \mathbf{1}_z) \Phi_{l,m}, \quad (l \neq 0 \text{ or } m \neq 0)$$

$$\sum_n (\mathbf{k}_{0,0,n} \cdot \mathbf{1}_z) \psi_{0,0,n} = (\mathbf{h}_{0,0} \cdot \mathbf{1}_z) (\Phi_{0,0} - 1). \quad (10)$$

The $\Phi_{l,m}$'s may be eliminated from Eqs. (9) and (10) and we obtain

$$\sum_n [(\mathbf{k}_{l,m,n} - \mathbf{h}_{l,m}) \cdot \mathbf{1}_z] \psi_{l,m,n} = 0, \quad (l \neq 0 \text{ or } m \neq 0) \quad (11)$$

$$\sum_n [(\mathbf{k}_{0,0,n} - \mathbf{h}_{0,0}) \cdot \mathbf{1}_z] \psi_{0,0,n} + 2(\mathbf{h}_{0,0} \cdot \mathbf{1}_z) = 0.$$

D. Numerical Solution

Let us assume that the sums appearing in Eqs. (4'), (5'), and (11) are truncated such that the numbers of values of l, m, n retained are equal to L, M, N , respectively. In this case, the number of equations contained in (5') and (11) is $L \cdot M \cdot (N+1)$, whereas the number

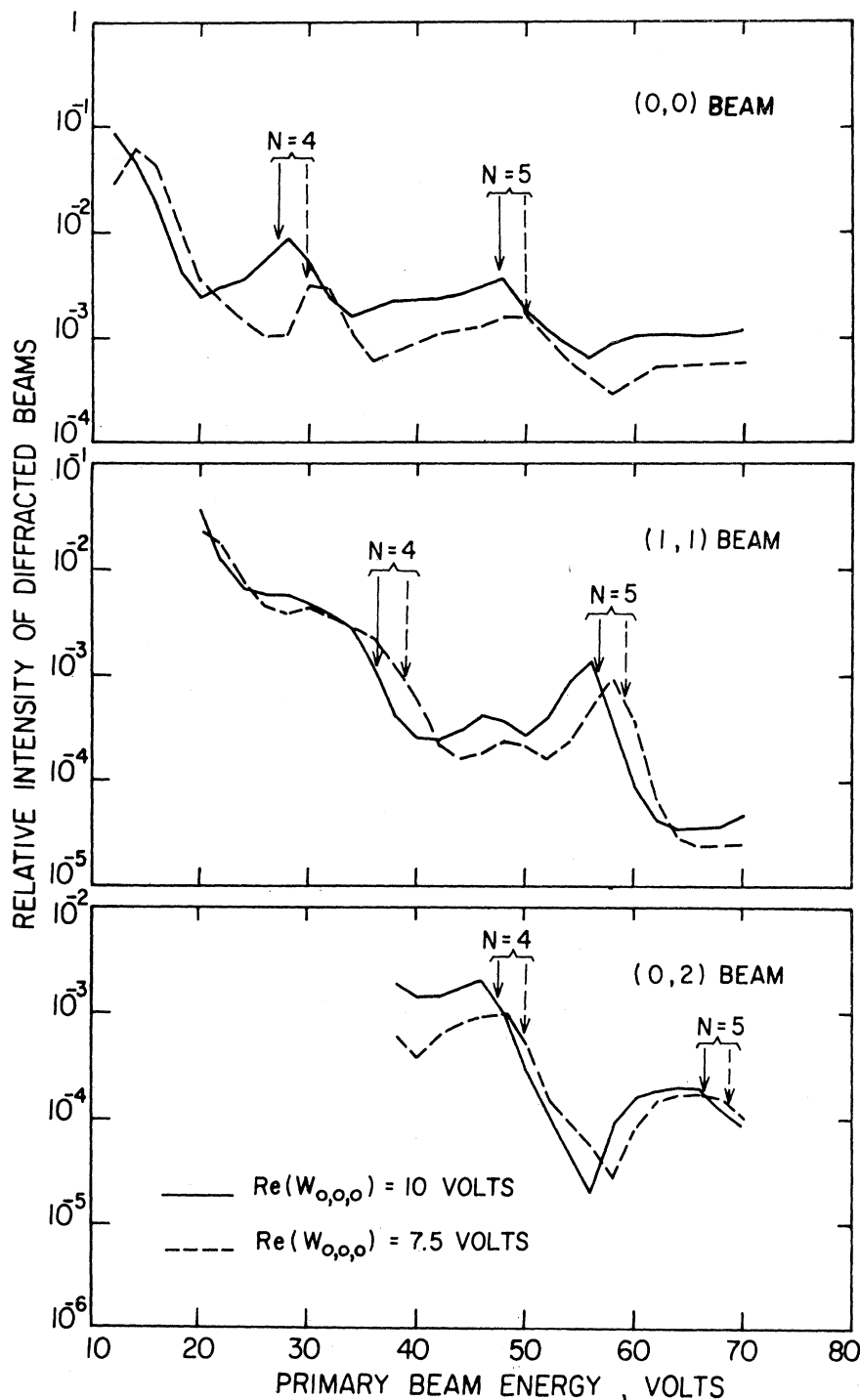


FIG. 1. Calculated beam intensities versus energy, showing the dependence on the inner potential. Conditions: imaginary part of potential $\text{Im}(w_{0,0,0}) = 2.5$ V; elastic scattering cross-section scaling factor = 1.0. The arrows indicate Bragg reflections of order N where the inner potential correction has been included. Beams with mixed indices are absent because of symmetry of the fcc lattice.

of unknowns is $L \cdot M \cdot N$. The problem is overdetermined because we are using a single Bloch wave to approximate the wave function in the crystal. Equations (5') and (11) may be written as one single matrix equation

$$G\psi = \mathbf{H}, \quad (12)$$

where G has L, M, N columns and $L, M, (N+Z)$ rows, ψ is an L, M, N dimensional vector containing the coefficients $\psi_{l,m,n}$, and \mathbf{H} is an $L, M, (N+1)$ dimensional vector. G and \mathbf{H} are known.

We now propose that an approximate solution of (12) may be found, according to the principle of least squares,

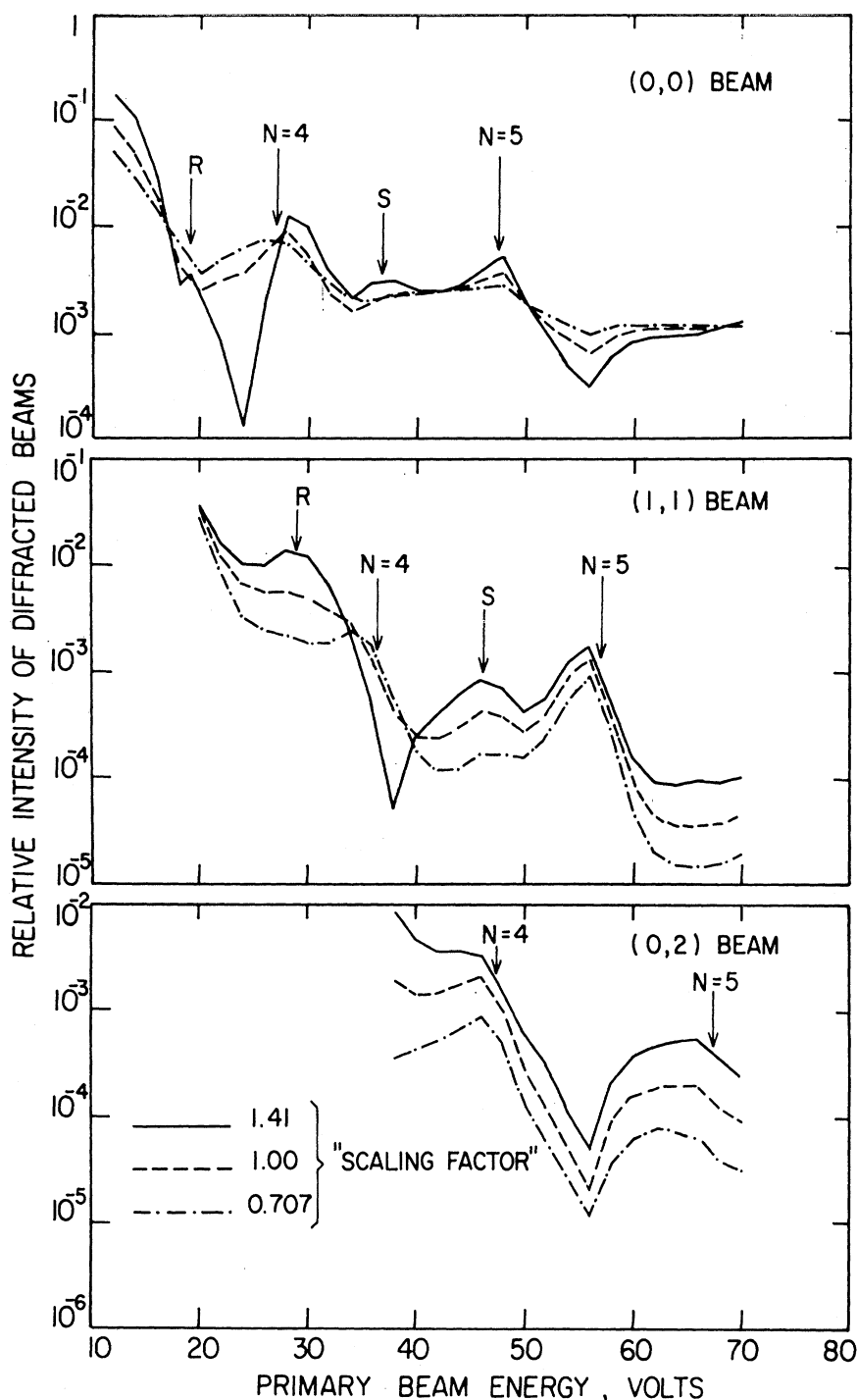


FIG. 2. Calculated beam intensities versus energy, showing the dependence on the elastic scattering cross section (scaling factor). Conditions: inner potential $\text{Re}(w_{0,0,0}) = 10$ V; imaginary part of the potential $\text{Im}(w_{0,0,0}) = 2.5$ V. The order of the Bragg reflections is indicated by N . S and R designate secondary Bragg and resonance peaks.

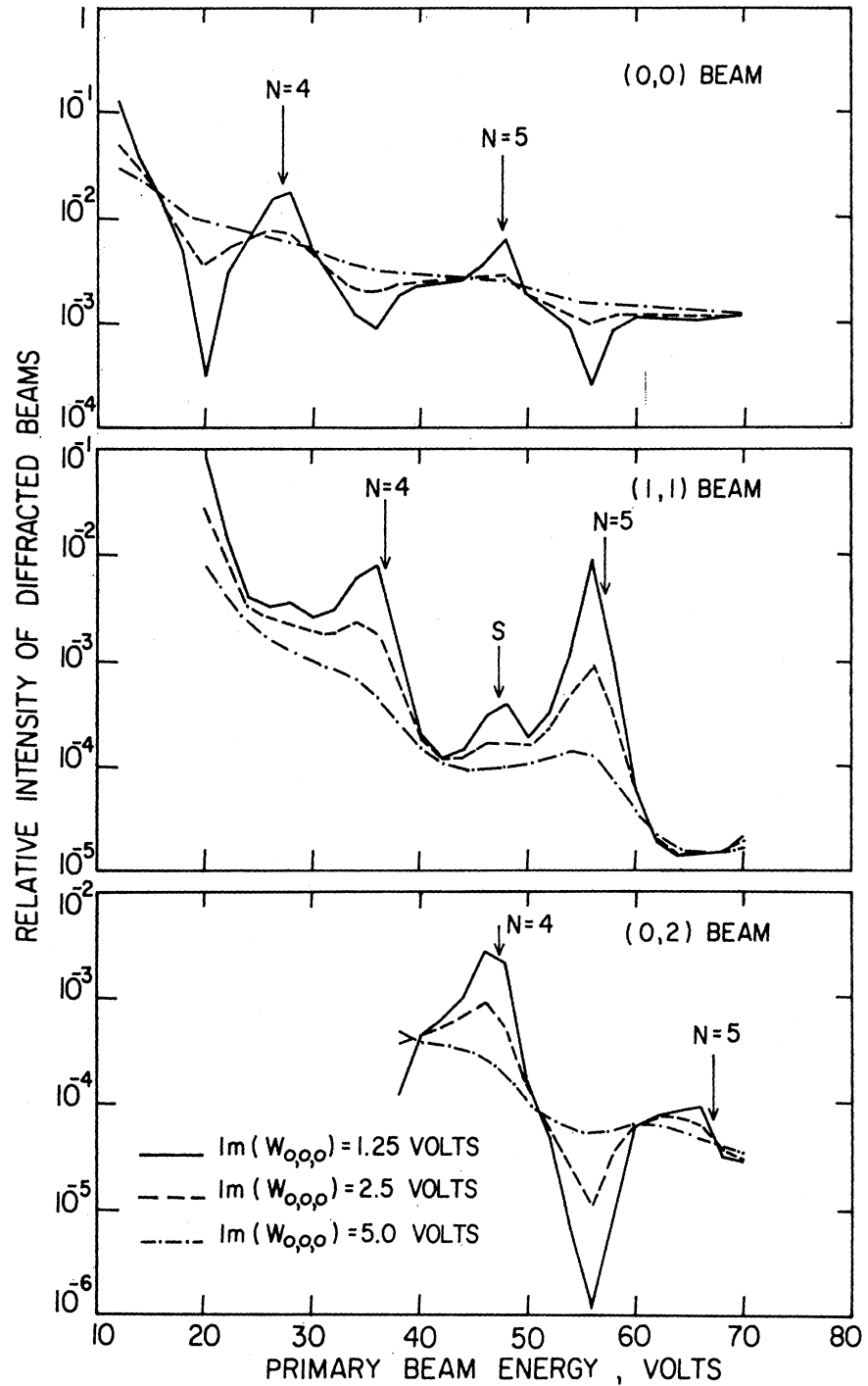


FIG. 3. Calculated beam intensities versus energy, showing the dependence on the imaginary potential. Conditions: inner potential $\text{Re}(w_{0,0,0}) = 10$ V; scaling factor = 0.707. N indicates the order of the Bragg reflections; S denotes a secondary Bragg peak.

by minimizing the quantity

$$S = (G\psi - \mathbf{H}) \cdot D(G\psi - \mathbf{H})^*, \quad (13)$$

where D is a positive, real, diagonal matrix, containing suitable weighting coefficients, and $*$ indicates complex conjugation. Since S is positive and quadratic in any of the unknown, $\text{Re}(\psi_{l,m,n})$ and $\text{Im}(\psi_{l,m,n})$, the mini-

mum is characterized by the conditions

$$\frac{\partial S}{\partial \text{Re}\psi_{l,m,n}} = 0, \quad \frac{\partial S}{\partial \text{Im}\psi_{l,m,n}} = 0, \quad (\text{any } l, m, n) \quad (14)$$

or, equivalently, in matrix form,

$$P\psi = \mathbf{Q}, \quad (15)$$

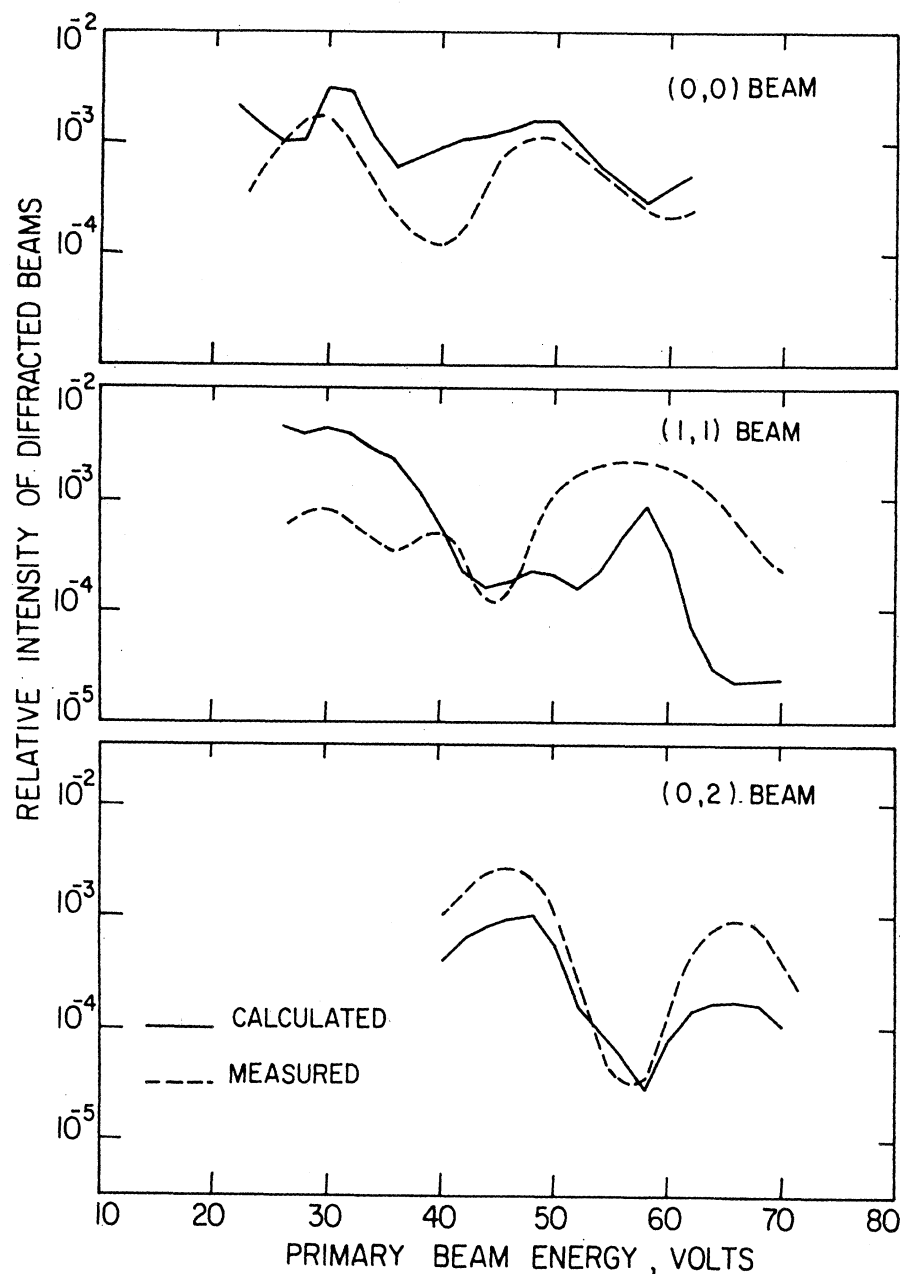


FIG. 4. Comparison between measured (Ref. 12) and calculated beam intensities versus energy. Theoretical conditions are as noted in Fig. 1 and experimental conditions are aluminum (100) surface, normal incidence.

where P is now a square matrix. Equation (15) is solved, not by straightforward inversion of P , but by an iterative technique that is not affected by round-off errors during the computation. Clearly, the result depends on the choice of D . However, in all cases that we have studied, this dependence turns out to be quite weak, because of the fact that the problem is only "slightly overdetermined," and, hence, there exists an "almost exact" solution of Eq. (12). We have investigated the influence of the relative magnitudes of the elements of D on the final result and found it to be negligible. For all our computations we therefore chose $D=I$ (unit matrix).

Obviously, once the vector ψ is known, the intensities of the diffracted beams, i.e., $|\tilde{\Phi}_{l,m}|^2$, are readily computed from Eqs. (9) and (10).

V. BEAM INTENSITY CALCULATIONS

Using the theory outlined above, calculations were performed under the following conditions:

- (1) A primary electron beam of unit intensity is incident normally on the (100) surface of an fcc lattice, with lattice constant, $a=4.04 \text{ \AA}$ (aluminum).
- (2) The crystal lattice is represented by a complex

potential. The shape of its real part, i.e., the relative magnitude of the expansion coefficients, $w_{l,m,n}$ [Eq. (1)], is obtained by Fourier-analyzing the "self-consistent" aluminum potential given in Ref. 8. The expansion includes all terms for which $l^2+m^2+n^2 < 4$, and the imaginary part of the potential is assumed independent of position and electron energy.

(3) The crystal surface, where the potential abruptly drops to zero, lies half-way between two layers of atoms.

(4) The wave function in the crystal is approximated by a single Bloch wave whose expansion is truncated such that $l^2+m^2+n^2 < 34$.

Figure 1 illustrates the dependence of the beam-intensity-versus-energy curves on the assumed inner potential ($Rew_{0,0,0}$). Decreasing the inner potential by 2.5 V translates the curves to a commensurate, higher energy.

Figure 2 shows the dependence of the beam intensities on the magnitude of the oscillatory part of the potential, i.e., on the elastic scattering cross section. The latter quantity is varied by introducing a scaling factor which multiplies all coefficients $w_{l,m,n}$, except $w_{0,0,0}$. For small cross sections, only the ordinary Bragg peaks are present. As the cross section is made larger, secondary Bragg peaks and resonance phenomena, due to multiple-scattering effects, appear.

Figure 3 demonstrates the dependence of the intensity curves on the magnitude of the imaginary potential, i.e., on the inelastic scattering cross section. As the imaginary potential decreases, the amount of "structure" (peak-to-valley ratios) increases considerably. This behavior is to be expected. A decrease in the inelastic scattering enhances the penetration of the primary beam and, therefore, enhances all three-dimensional effects. Clearly, the very existence of Bragg peaks or structure is a three-dimensional effect par excellence. The disappearance of the secondary Bragg peaks for large values of the imaginary potential, as seen in Fig. 3., indicates that these peaks may be attributed to multiple-scattering events involving atoms in different layers, rather than atoms in a single layer.

VI. COMPARISON WITH EXPERIMENT

Beam intensity measurements on the (100) surface of aluminum single crystals are being performed by Bedair at our laboratory. Figure 4 compares his measurements¹² with a typical set of our theoretical curves. All three experimental curves are normalized to the same primary electron beam current. Intensity ratios between different beams are, therefore, represented correctly.

When considering this comparison between theory and experiment (Fig. 4.), the following points should be borne in mind:

(1) No attempt has been made to optimize the parameters of the potential, i.e., the expansion coefficients $w_{l,m,n}$.

(2) The imaginary part of the potential has been assumed constant, whereas it should vary with electron energy in order to represent the known variation of inelastic scattering cross sections with energy.

(3) The theoretical results reported here are based on a single-Bloch-function representation. It remains to be investigated whether this is a good approximation, or whether there are cases where a more rigorous multi-Bloch-function treatment must be used.

A thorough parameter optimization, along the lines indicated above, might improve the agreement between theory and experiment considerably. This would, however, represent a very large investment in computer time.

VII. CONCLUSIONS

We have shown that an extended Bethe theory may be applied successfully to the computation of LEED intensities. The results are in reasonable agreement with measured¹² beam intensities (Fig. 4.), although we have used a single-Bloch-function approximation in order to avoid an excessively lengthy calculation, and although there are at least two limitations inherent in our model which have to be seriously questioned.³ These are the use of an incident plane wave and the assumed perfect periodicity with abrupt cutoff at the crystal surface.